

Received November 24, 2019, accepted December 10, 2019, date of publication December 23, 2019, date of current version December 31, 2019.

Digital Object Identifier 10.1109/ACCESS.2019.2960828

Super Resolution Reconstruction of Images Based on Interpolation and Full Convolutional Neural Network and Application in Medical Fields

NA SUN¹ AND HUINA LI²

¹School of Information Engineering, Minzu University of China, Beijing 100081, China

²School of Information Engineering, Xuchang University, Xuchang 461000, China

Corresponding author: Na Sun (sunna_07@muc.edu.cn)

ABSTRACT The traditional image to enlarge algorithms include nearest neighbor interpolation, bilinear interpolation and high-order interpolation. In order to achieve super-resolution reconstruction of images, a new algorithm combining traditional algorithms and deep learning is proposed. The framework is divided into two parts. Firstly, the deep reconstruction of the low-resolution data is performed by the ability of deep learning to extract features automatically. Then, combining with the traditional interpolation reconstruction results, the deep learning algorithm is used again for training and learning, and finally the high-resolution reconstructed data is obtained. The algorithm is validated using an online public test data set. The results show that the algorithm has a significant effect on the MSE (mean squared error) and PSNR (Peak Signal to Noise Ratio). Compared with the traditional interpolation algorithm and the single deep learning algorithm, the proposed algorithm has higher performance. Moreover, the proposed algorithm is perfect for the reconstruction of the details, the outline is clear, and the high-quality image is obtained.

INDEX TERMS Interpolation, deep learning, super-resolution, reconstruction, MSE, PSNR.

I. INTRODUCTION

Super resolution reconstruction is to restore high resolution images from low resolution images or image sequences. High resolution image means that the image has more detailed information and more exquisite picture quality, which has important application value in the fields of high-definition television, medical image, remote sensing satellite image, etc. We enlarge the specific image to make the image still clear and retain more details.

In the process of digital image acquisition, due to the influence of many factors such as atmospheric disturbance and defocusing, the quality of the collected images will decline to different degrees. In addition, the noise introduced in the imaging process will further aggravate the image degradation. With the significant improvement of computer technology and computer performance, people have higher requirements for the image quality. However, due to the limitations of environment and hardware, the quality of the collected images is not as good as expected. This led to the idea of improving the resolution of images by improving the hardware, software or

environment. If the resolution of the image is improved by improving the hardware, the cost will be very high. If the resolution of the image is improved by improving the environment, it is difficult to achieve in practice and may cause greater losses. Therefore, software is usually used to improve the resolution of images. The super resolution algorithm of images is to generate corresponding high-resolution images from known low-resolution images.

In the field of entertainment, many composite images are used in the design of film and television works. In the medical field, with the development of technology and medical image engineering, many advanced imaging devices have been applied in the medical field, which provides a variety of images for clinical diagnosis and further promotes the progress of modern clinical technology. In the industrial field, image processing technology can be used to classify and identify industrial parts in some toxic environments. In the field of earthquakes, the staff can analyze and process seismic images, making it easier for translators to discover and identify geological features and make timely and accurate geological interpretations. Therefore, the research on image processing technology has a very important practical value.

The associate editor coordinating the review of this manuscript and approving it for publication was Wei Wei.

Traditional techniques of super resolution reconstruction and amplification for images generally include interpolation-based super-resolution reconstruction, reconstruction-based super resolution reconstruction and learning-based super resolution reconstruction. Image amplification as a modern image processing technology is playing an important role in practical application. Meanwhile, it also has a lot of special advantages especially in many multidisciplinary, such as medical, aerospace, crime detection and image processing software “PHOTOSHOP”. It can be seen that the core goal of image amplification is to obtain a better visual effect after enlarging a digital image. However, image amplification is a hot spot in image processing, and improving image quality is the main goal of image amplification algorithms.

We will combine traditional interpolation algorithms with the algorithm based on deep learning, propose a new kind of super resolution reconstruction algorithm. The traditional interpolation algorithm mainly includes the nearest neighbor interpolation, linear interpolation and so on. Based on the study of interpolation, the purpose of image zooming or improving the quality is achieved. Then the result of traditional interpolation and initial reconstruction are combined to train the deep learning. Finally, online public data sets are used to validate the proposed algorithm.

Section II introduces some basic interpolation algorithms and the research of super-resolution reconstruction. Section III introduces the proposed algorithm. Section IV is the experimental part, which verifies the effectiveness of the proposed algorithm through different data sets. Section V is the conclusion, which summarizes findings and contributions.

II. RELATED WORK

A. SUPER RESOLUTION RECONSTRUCTION FOR IMAGES BASED ON INTERPOLATION

By means of the values of several known points around a certain point, as well as the position relations between the surrounding points and the point, according to a certain formula, the interpolation method is used to calculate the value of the point. There are many interpolation methods. The common interpolation algorithms are nearest neighbor interpolation, bilinear interpolation, cubic interpolation and so on.

The nearest neighbor interpolation algorithm is the simplest interpolation algorithm among several interpolation algorithms [1]. The output pixel value is the pixel value of the input image and its nearest sampling point. For example, Figure 1 is the nearest interpolation effect diagram, where the point A_0 is mapped to A_1 in set transformation. However, since the point A_1 is in the coordinate position of non-integer, the pixel gray value cannot be extracted, so the gray value of the nearest sampling point A_2 can be approximated as the gray value of A_0 .

In many image processing software, the nearest neighbor interpolation algorithm is adopted to enlarge and transform the image. It can be seen from the form that its calculation is simple, and the output effect is very good in many

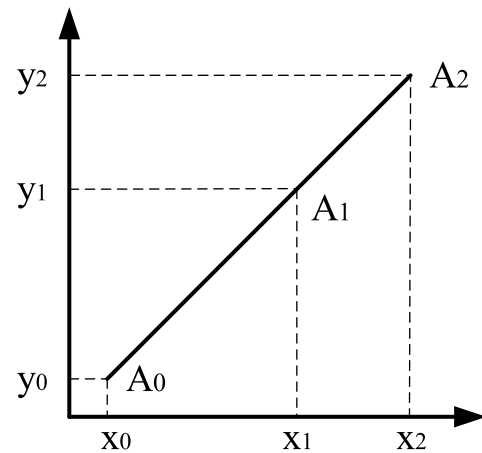


FIGURE 1. Nearest neighbor interpolation effect.

cases, which can be accepted by most people, so this algorithm is widely used in many commercial software. However, the nearest neighbor interpolation algorithm can produce so-called machining marks in the image.

Generally, digital image scaling refers to scaling a given image in the same direction x and direction y to obtain a new image, also known as full scale. If the scale of the amplification is different in direction x and direction y , the scale of the image will change the relative position between the pixels of the original image, resulting in geometric deformation. Suppose the point $A_0(x_0, y_0)$ in the original image is scaled to scale, and in the new graph it is corresponding point $A_1(x_1, y_1)$, then the coordinate relation between $A_0(x_0, y_0)$ and $A_1(x_1, y_1)$ can be expressed as:

$$\begin{bmatrix} x_1 \\ y_1 \\ 1 \end{bmatrix} = \begin{bmatrix} a & 0 & 0 \\ 0 & a & 0 \\ 0 & 0 & 1 \end{bmatrix} \begin{bmatrix} x_0 \\ y_0 \\ 1 \end{bmatrix} \tag{1}$$

In other words, its coordinates are transformed like the following:

$$\begin{bmatrix} (0, 0) \rightarrow (0, 0) \\ (0, 1) \rightarrow (0, 2) \\ (0, 2) \rightarrow (0, 4) \\ (0, 3) \rightarrow (0, 6) \\ (1, 0) \rightarrow (2, 0) \\ \dots \\ (3, 0) \rightarrow (6, 0) \\ (3, 1) \rightarrow (6, 2) \\ (3, 2) \rightarrow (6, 4) \\ (3, 3) \rightarrow (6, 6) \end{bmatrix} \tag{2}$$

Bilinear interpolation is to use the pixel values of the four adjacent points ($g(0, 0)$, $g(0, 1)$, $g(1, 0)$, and $g(1, 1)$) around the original image p to perform linear interpolation in the two directions of x and y , as shown in Figure 2.

The interpolation algorithm uses a piecewise linear function to approximate the contribution of the gray value of the four adjacent points to the gray value of the inner

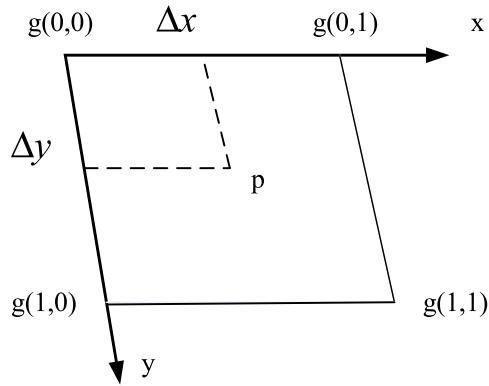


FIGURE 2. Bilinear interpolation method.

interpolation point. The piecewise linear function is:

$$\omega(t) = \begin{cases} 1 - |t|, & 0 \leq |t| \leq 1 \\ 0, & \text{others} \end{cases} \quad (3)$$

Suppose the interval between pixels in Figure 2 is 1, and the projection of the distance from point p to pixel $g(0, 0)$ in the x and y directions is Δx and Δy , then the gray value of interpolation points p is

$$D_p = [\omega(\Delta x)\omega(1 - \Delta x)] \begin{bmatrix} D_{00} & D_{01} \\ D_{10} & D_{11} \end{bmatrix} \begin{bmatrix} \omega(\Delta y) \\ \omega(1 - \Delta y) \end{bmatrix} \quad (4)$$

where, D_{ij} is the gray value of pixel $g(i, j)$. Both bilinear interpolation and cubic interpolation algorithms can get clear target images by resampling according to scaling requirements, but the cubic interpolation algorithm has relatively high complexity.

Jensen and Anastassiou [2] used some templates to detect and fit edges to improve the visual appearance of super-resolution results. Muresan *et al.* [3] have detected edges in diagonal and off-diagonal directions and then generated high-resolution images using one-dimensional polynomial interpolation functions along the edge. Li and Orchard [4] proposed an interpolation algorithm based on edge guidance. Based on geometric duality, the local covariance of high-resolution images was estimated by low-resolution localization. The information can reflect the edge direction information of the image, which can be used to guide the interpolation of high resolution images. Hung and Siu [5] proposed a weighted-based least squares estimation method, which optimizes and improves the interpolation result by the geometric similarity of pixels and the weight of bilateral filters.

Dong *et al.* [6] and Zhang *et al.* [7] introduced the idea of non-local means (NLM), extending the concept of local regions to the entire image space, using these repetitive structures for non-local interpolation, and displaying when the amplification is large. Wong and Siu [8] proposed a method of adaptive orientational Windows selection (ADWS) for the edge-guided interpolation algorithm by adopting a fixed window and not completely analyzing the edge information.

By considering the directional ellipse window, the edge letter is utilized. The suffocation finds the optimal window as the sample point in the Wiener filter, thereby greatly reducing the ringing effect present in the interpolated image. Mishiba *et al.* [9] used an edge-based adaptive smoothing filter based on the observation model to constrain the interpolated image with edge-oriented smoothness and fidelity to the original low-resolution image data by solving the least squares problem of constraints, get high resolution images. Cascida *et al.* [10] further optimized the edge-directed interpolation algorithm by using adaptive anisotropic radial basis functions.

Mallat and Yu [11] proposed a new idea of sparse mixed estimation in 2010. This method innovatively proposes a new adaptive estimator. The estimator is composed of a series of linear inverse estimators and the mixing coefficient of the estimator is calculated in the coefficient block. The method introduces a fast-orthogonal tracking block matching algorithm, which not only improves the efficiency but also produces clearer high-resolution images. Zhou *et al.* [12] proposed an interpolation algorithm based on surface fitting. This algorithm uses multi-surface fitting to make full use of spatial structure information. A curved surface is constructed at each low resolution pixel and the least square algorithm is used to minimize the fitting error. In the absence of any priori, the interpolation algorithm based on surface fitting can effectively reduce the stepped boundary phenomenon and retain the details of the image. In general, the interpolation algorithm is simple to implement, but the high-resolution images it produces are not ideal. With the addition of edge guidance and other algorithms, it is still not possible to estimate the high frequency part of the high-resolution image, and it is easy to make the image too smooth and even blur the details and edges of the image.

B. SUPER RESOLUTION RECONSTRUCTION TECHNOLOGY BASED ON DEEP LEARNING

Convolutional Neural Network (CNN) is a feedforward neural network, whose artificial neuron can respond to the peripheral neurons in a partial coverage range and has excellent performance in large image processing. At present, it has become a research hotspot in many fields. CNN is a network structure of weight sharing. Compared with MLP (Multilayer Perceptron) [13], DBN (Deep Belief Network) [14] and other neural networks, it has fewer adjustable parameters and reduces the learning complexity. When processing two-dimensional images, CNN has a stable status for translation, tilt, zoom, or other forms of deformation.

CNN can be traced back to decades ago [15]. Due to its success in image classification [16] and [17], it has been widely popular. They have also been successfully applied in other computer vision fields, such as target detection [18], [19], face recognition [20], pedestrian detection [21] and so on. There are several important reasons for the progress: (1) powerful GPU can achieve an effective training [17]; (2) the

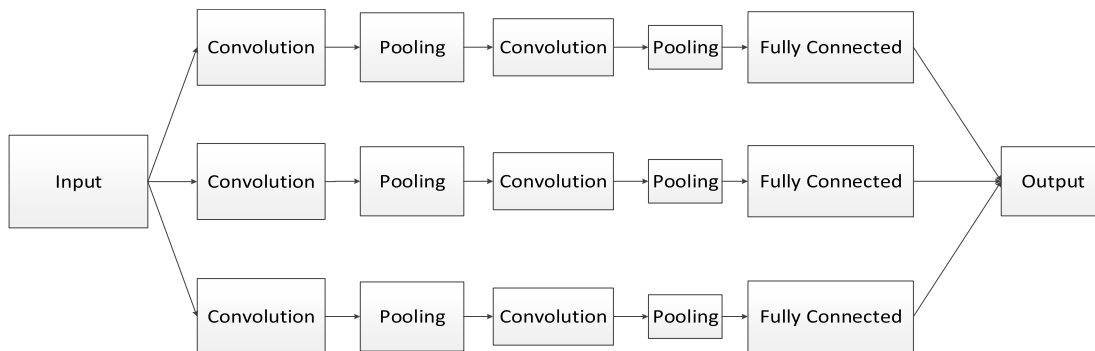


FIGURE 3. Structure diagram of the traditional CNN.

proposed modified linear element (Rectifier Linear Unit, ReLU) [22] makes convergence faster. Figure 3 shows the traditional CNN structure, which includes the input layer, convolution layer, pooling layer, full connection layer and output layer. CNN on regularization method of learning and has made considerable progress, including ReLU, the number of standardization (Batch Normalization, BN) and residual learning.

Super-resolution reconstruction is an inverse problem. For a low-resolution image, there may be many different high-resolution images corresponding to it. Therefore, a prior information is usually added to normalize the solution of high-resolution images. In the traditional method, the information can be learned from several pairs of low-high resolution images. Deep learning-based super-resolution reconstruction directly learns the end-to-end mapping function from high-resolution image to high-resolution image through neural network.

In the field of image reconstruction, learning-based method is a hotspot in recent years. The end-to-end nonlinear mapping between high and low resolution images is achieved by learning. Chang et al proposed neighborhood embedding method [23], [24], which solved learning parameters through k adjacent values of low-resolution image blocks, reducing the dependence on sample values in the reconstruction process. Anchor neighborhood regression method was proposed by Timofte *et al.* [25], which can effectively reduce the complexity of the algorithm by calculating the neighborhood of dictionary atoms. The sparse representation proposed by Yang *et al.* [26] establishes complete dictionary pairs for high and low resolution respectively, and then obtains high-resolution image blocks through sparse expression coefficients in low-resolution dictionaries, forming feature mappings between images. Inspired by the end-to-end mapping of sparse coding, Dong *et al.* [27] applied the 3-layer neural network to directly learn the feature mapping between high and low resolution, extracted the features successively by CNN and carried out the linear mapping, and finally carried out the high-resolution reconstruction. In addition, in recent years, neural network models such as ARCNN [28], residual neural network [29] and VDSR algorithm [30] based

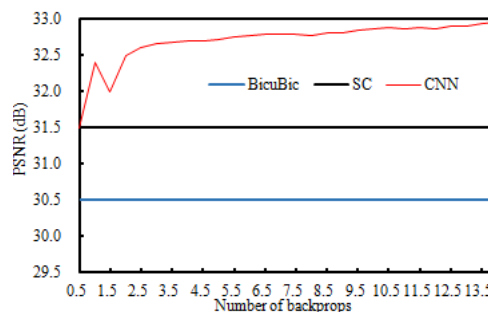


FIGURE 4. Performance comparison of three kinds of algorithms.

on VGG network have achieved good reconstruction results, but the disadvantages are large number of parameters and high model complexity.

In order to solve these problems, we propose to combine the traditional interpolation algorithm with the deep learning theory, and use the simple three-layer CNN combining with the interpolation algorithm to complete the super-resolution reconstruction, and achieve an ideal effect.

III. METHOD

Combining with the idea of deep learning, we propose a super-resolution reconstruction structure combining the interpolation algorithm and FCN (Fully Convolutional Neural Network). The network directly learns the mapping between low resolution and high resolution images end-to-end, no pre-processing and post-processing. First, its structure is intentionally simple, but it provides greater precision than the most advanced instance-based methods. Figure 4 shows an example comparison. Secondly, through appropriate filters and layers, the image can be enlarged, and the image details will be clearer. It still works on the CPU. As the number of iterations increases, the PSNR of the deep learning algorithm increases all the time, while the traditional method is not changing.

The CNN we used has five layers:

the first layer is the input layer, and the size of the input image is $200 \times 300 \times 3$;

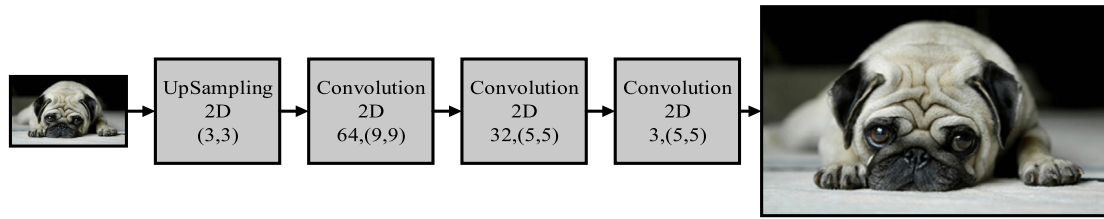


FIGURE 5. Network structure diagram.

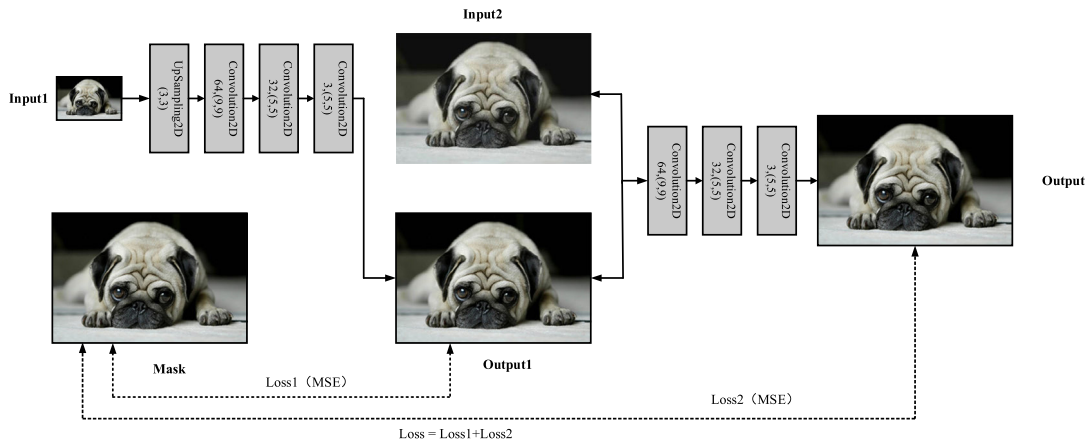


FIGURE 6. The combined network structure of interpolation and full convolutional neural network.

since the function we realized is image amplification, we set the upper sampling layer as the second layer and the sampling step size as 3 to realize image amplification function;

the third layer is set as convolution layer, the size of convolution kernel is 9×9 , and the number of convolution kernel is 64;

the fourth layer is set as convolution layer, the size of convolution kernel is 5×5 , and the number of convolution kernel is 32;

the fifth layer is set as the convolution layer, as the output layer of the network. The size of convolution kernel is 5×5 . Since the training data of the network are color images, the number of convolution kernel is 3, which is the three channels of color image (R, G, B).

The proposed network structure is shown in Figure 5.

The end-to-end learning mapping functions require estimating a range of network parameters. This is done by minimizing the loss between the reconstructed image $f(x)$ and the real corresponding real image $g(x)$. Mean Squared Error (MSE) is used as the loss function:

$$L(\Theta) = \frac{1}{n} \sum_{i=1}^n \|f(x) - g(x)\|^2 \quad (5)$$

where, n is the number of training samples, and the use of MSE as a loss function is conducive to obtaining a high Peak Signal to Noise Ratio (PSNR). PSNR is a widely

used quantitative index to evaluate image restoration quality, which is at least partially related to perceived quality. It is worth noting that the CNN does not exclude the use of other types of loss functions, as long as the loss function is differentiable. If a better loss function is given in the training process, then the network can flexibly adapt to this measure. In contrast, with traditional manual methods, this flexibility is often difficult to achieve.

We use the Adam (Adaptive Moment Estimation) minimization reconstruction loss function, which automatically adjusts the learning rate and converges faster and performs better in complex networks. In order to improve the effect of super resolution reconstruction, we combine the traditional interpolation algorithm with the full convolution method, and propose the network structure shown in Figure 6.

Our proposed network consists of two parts. In order to reduce the data dimension and reduce the influence of redundant features, the traditional CNN structure sets a pooling layer after the convolution layer to reduce the data dimension and improve the speed of model training. In our method, we do not set the pooling layer in each structure. Although the pooling layer reduces the dimension, it also removes some features, which may affect the final results.

The network structure we designed is shown in Figure 6. The network consists of two inputs, one for low-resolution image and the other for interpolation. The network first samples low-resolution images, then extracts features through the convolution layer, then combines the output and interpolation

results, and then extracts features by the convolution layer. Finally, the output is high resolution and enlarged image. The first part is the initial super-resolution reconstruction with the same structure as Figure 5. The second part combines interpolation output with network output. As the output of the second network structure, this part includes three convolution layers:

the size of convolution kernel is 9×9 , and the number of convolution kernel is 64.

the size of convolution kernel is 5×5 , and the number of convolution kernel is 32;

the size of convolution kernel is 5×5 , and the number of convolution kernel is 3. This layer serves as the output of the whole network.

Loss function: we set two MSE as loss functions to optimize the network structure together.

$$L(\Theta) = \frac{1}{n} \sum_{i=1}^n \|f_1(x) - g(x)\|^2 + \frac{1}{n} \sum_{i=1}^n \|f(x) - g(x)\|^2 \quad (6)$$

where, $f_1(x)$ is the output result of the first part.

IV. EXPERIMENTAL

The experimental platform is PyCharm, using keras and TensorFlow port, the computer is configured as Inter(R) Core(TM) i7-8750H @2.20GHz, 16GB memory, Nvidia GeForce GTX 1070 GPU, using 64 bit Win10.

Our data sets come from public databases and online downloads. Four data sets were selected to test the proposed model, namely the Berkeley Segmentation Dataset (BSDS), ImageNet Dataset, BrainWeb, and Middlebury Dataset [31], [32]. Among them, BSDS data set is mainly used for image segmentation and boundary detection, and is often used for image resolution reconstruction, which is characterized by obvious edge features and less noise. In this experiment, 200 and 91 images of different scenes were randomly selected from BSDS and ImageNet to form the 291 image samples required for this experiment. A total of 1, 778 images were obtained using publicly available data downloaded from the Internet. In order to utilize unified analysis, we set the image size uniformly to $300 \times 300 \times 3$, and then reduced the image size by three times to $(100 \times 200 \times 3)$ as the input image. The original image is the real label image. In terms of preprocessing, we normalize the image pixels to between (0, 1). 1500 of the 1778 images were used as training set, and the remaining 278 images were used as test images. Figure 7 shows the randomly selected input and real images.

We used five kinds of algorithms for image amplification, namely nearest neighbor interpolation algorithm, bicubic interpolation algorithm, FCN algorithm, FCN + nearest neighbor interpolation, FCN + bicubic interpolation.

We analyze the five algorithms from objective and subjective aspects. In terms of subjective evaluation, we directly evaluate the effectiveness of the algorithm based on the visual effect after processing. In terms of objective evaluation, MSE and PSNR were used as evaluation indexes to objectively evaluate the method.

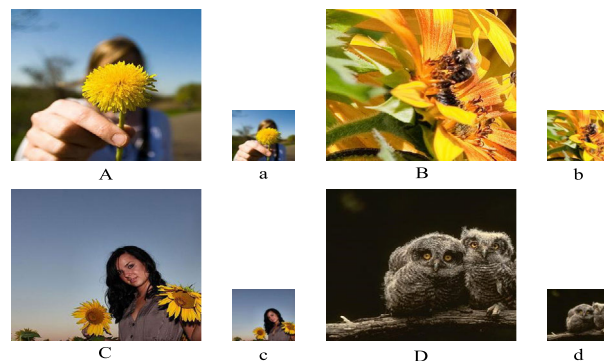


FIGURE 7. A, B, C and D are the real images, while a, b, c and d are the images reduced by three times.

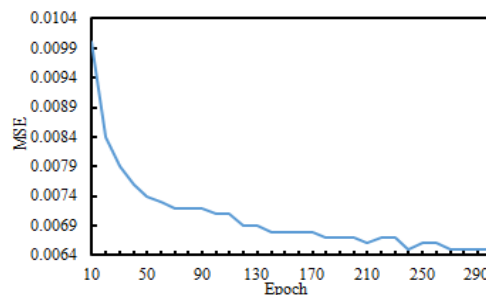


FIGURE 8. The learning process of MSE.

Evaluation criteria: in this paper, the PSNR and MSE were selected as objective evaluation indexes for reconstruction quality. PSNR value can measure the error between pixels of corresponding points, and the computed results are related to the MSE. The larger the value of PSNR is, the smaller the distortion is. If the size of X and Y of the two comparison images input are both $H \times W$, then:

$$MSE = \frac{1}{H \times W} \sum_{i=1}^H \sum_{j=1}^W (X(i, j) - Y(i, j))^2 \quad (7)$$

$$PSNR = 10 \log_{10} \left(\frac{(2^n - 1)^2}{MSE} \right) \quad (8)$$

where, X (i, j) is the pixel value of row i and column j of the input image; Y (i, j) is the pixel value of row I and column j of the reference image; H and W are the height and width of the image.

As shown in Figure 8, the learning process of the loss function in the training process is presented. With the increase of the number of iterations, MSE keeps decreasing and finally tends to be flat.

Experiment 1: nearest neighbor interpolation algorithm.

We first processed the test set with the nearest neighbor interpolation algorithm, and the experimental results are shown in Figure 9, and MSE and PSNR are shown in Table 1.

It can be seen from Figure 9 that recently interpolation, as a traditional super-resolution reconstruction method, does not maintain the image details very well, and the main details are

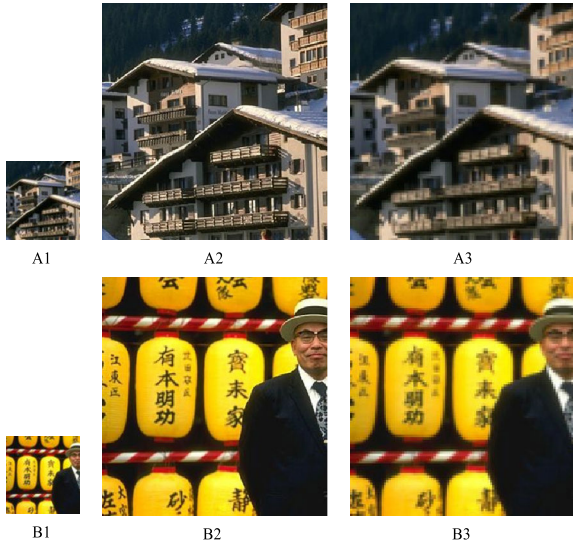


FIGURE 9. A1 and B1 are input images, A2 and B2 are real images, A3 and B3 are enlarged images.

TABLE 1. MSE and PSNR of nearest neighbor algorithm.

	MSE	PSNR
A3	0.01019	19.9144
B3	0.00478	23.2028

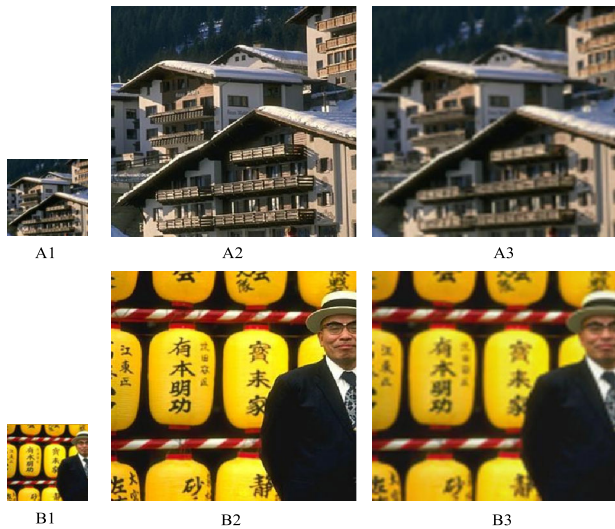


FIGURE 10. A1 and B1 are input images, A2 and B2 are real images, A3 and B3 are enlarged images.

blurred. It can be seen from Table 1 that the PSNR of the two images is low and the processing effect is not very ideal.

Experiment 2: bicubic interpolation algorithm.

The experimental results are shown in Figure 10, and MSE and PSNR are shown in Table 2.

Comparing experiment 2 with experiment 1, it can be seen from Figure 10 that the blurring phenomenon is greatly reduced, the PSNR is improved, and the MSE is reduced. However, the blurring phenomenon still exists in the image.

TABLE 2. MSE and PSNR of Bicubic interpolation algorithm.

	MSE	PSNR
A3	0.00868	20.6124
B3	0.00304	25.1696

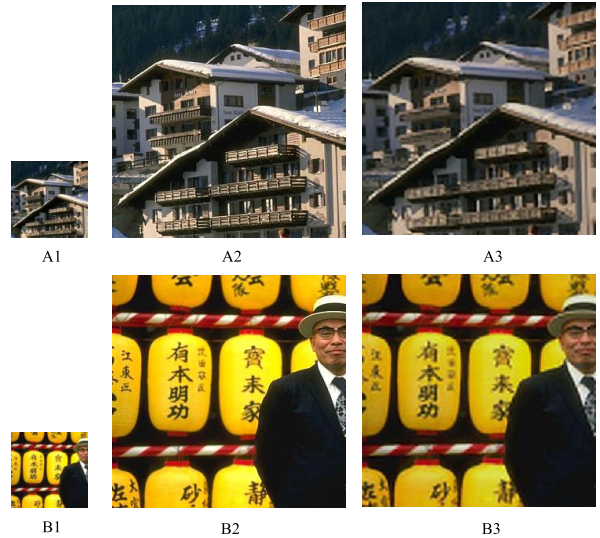


FIGURE 11. A1 and B1 are input images, A2 and B2 are real images, A3 and B3 are enlarged images.

TABLE 3. MSE and PSNR of deep learning algorithm.

	MSE	PSNR
A3	0.007451	21.2775
B3	0.002189	26.59621

TABLE 4. MSE and PSNR of FCN+ nearest neighbor algorithm

	MSE	PSNR
A3	0.00709	21.4893
B3	0.00200	26.9799

Experiment 3: super resolution reconstruction algorithm based on FCN.

Experimental results are shown in Figure 11, and MSE and PSNR are shown in Table 3.

We compare the experimental results of deep learning algorithm with those of experiment 1 and experiment 2. The MSE and PSNR of two images are improved, which proves the deep learning algorithm has the ability to obtain the super-resolution reconstruction. Meanwhile, the deep learning algorithm can achieve obvious effects than the traditional interpolation algorithm. Intuitively, it can be seen that deep learning approach to image details remain relatively perfect.

Experiment 4: FCN and nearest neighbor algorithm are combined.

Experimental results are shown in Figure 12. MSE and PSNR are shown in Table 4.

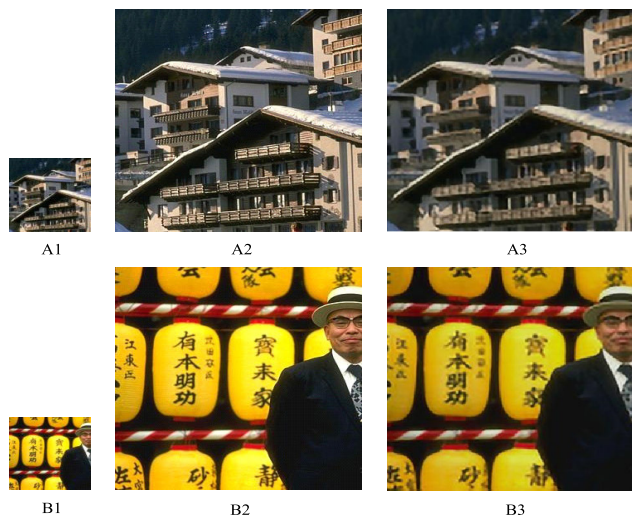


FIGURE 12. A1 and B1 are input images, A2 and B2 are real images, A3 and B3 are enlarged images.

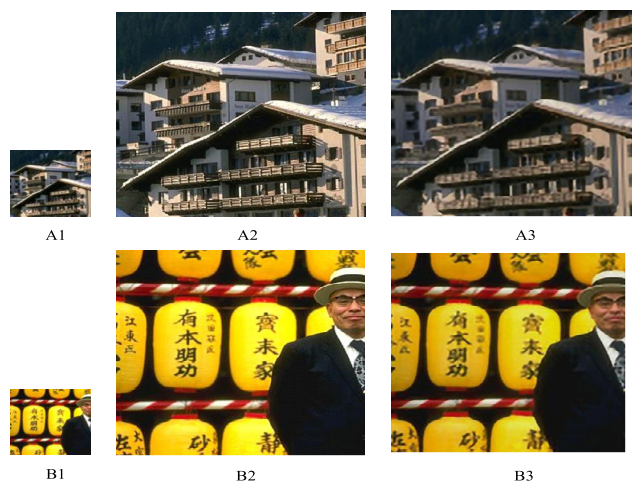


FIGURE 13. A1 and B1 are input images, A2 and B2 are real images, A3 and B3 are enlarged images.

TABLE 5. MSE and PSNR of FCN + Bicubic interpolation algorithm.

	MSE	PSNR
A3	0.00666	21.7597
B3	0.00171	27.6535

In this experiment, we combined the deep learning algorithm with the nearest neighbor interpolation algorithm to improve the super-resolution capability of the combination. The experimental results show that MSE and PSNR are improved after the combination with the nearest neighbor, and the effect is obvious, which can demonstrate the effectiveness of our proposed algorithm.

Experiment 5: FCN was combined with the bicubic interpolation algorithm.

Experimental results were shown in Figure 13. MSE and PSNR were shown in Table 5.

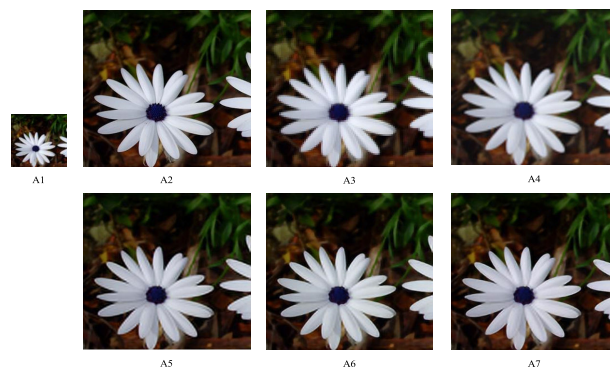


FIGURE 14. comparison of experimental results. A1 is input image, A2 real enlarged image, A3 nearest neighbor interpolation algorithm, A4 bicubic interpolation algorithm, A5 deep learning algorithm, A6 deep learning and nearest neighbor interpolation algorithm, A7 deep learning and bicubic interpolation algorithm.



FIGURE 15. comparison of experimental results. B1 is input image, B2 real enlarged image, B3 nearest neighbor interpolation algorithm, B4 bicubic interpolation algorithm, B5 deep learning algorithm, B6 deep learning and nearest neighbor interpolation algorithm, B7 deep learning and bicubic interpolation algorithm.

TABLE 6. Comparison of experimental results.

A	INTER _NEAREST	INTER _CUBIC	FCN	FCN +INTER NEAREST	FCN+ INTER CUBIC
MSE	0.00325	0.00191	0.00116	0.00088	0.00061
PSNR/dB	24.8707	27.1995	29.3409	30.5602	32.1382
B					
MSE	0.00157	0.00079	0.00045	0.00038	0.00026
PSNR/dB	28.04996	30.9823	33.4560	34.1578	35.7879

In order to further illustrate the proposed algorithm for super resolution reconstruction has significant improvement, we combine the deep learning algorithm with the bicubic interpolation algorithm.

It can be seen from Table 5, PSNR of the second image has reached 27.6535dB. Compared with experiments 1-4, the results obtained by this algorithm will be better in MSE and PSNR.

In order to clearly illustrate the algorithm we proposed, we randomly selected two images and compared the effects of five algorithms. Experimental results are shown in Figures 14 and 15. MSE and PSNR are shown in Table 6.

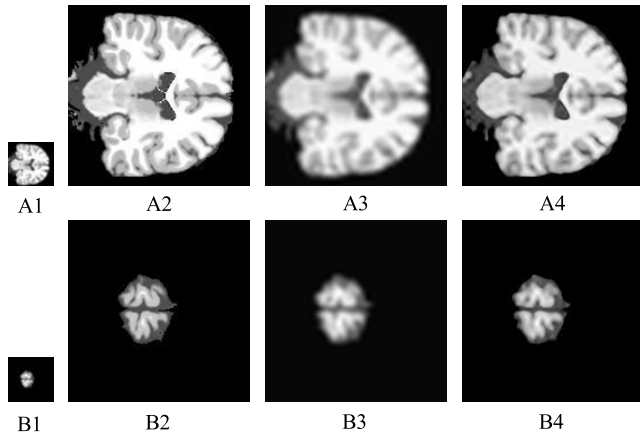


FIGURE 16. Medical image results, A1, B1 of the input image, A2, B2 is a real image, A3, B3 are the nearest neighbor interpolation results, A4, B4 are the enlarged results of the proposed algorithm.

As can be seen from Figures 14 and 15, A7 and B7 almost achieve the effect of real images. It can be seen from Table 6, no matter in MSE and PSNR, the proposed algorithm is the best. Therefore, the presented algorithm not only on the final quality reconstruction effect best, under the same number of iterations, also can get a better effect of super-resolution reconstruction. Compared with other algorithms, the proposed neural network model can recover more image details and has higher evaluation indexes. It can be explained that our proposed method provides a new idea for super resolution.

Experiment 6: To verify the validity of the proposed algorithm in medical field, we used MRI images of the brain to verify the effect. The dataset come from BrainWeb simulates brain datasets. There is 3D simulated MRI image as test data. This set of data consists of a multi-level real-time simulated MRI image of intensity non-uniformity and noise [31].

In the medical field, some acquired images are limited in size. For some older doctors, the images are too small and the resolution is low, so that useful details cannot be grasped in time. For the medical field, it is very important to enlarge the image without distortion.

We will amplify the image about four times, the original image is reduced as four times as the input low resolution image. In order to reduce the redundancy of the experiment, we did not use the above five algorithms to process the medical image, but the most appropriate method of the above five methods. From the above effect of natural image processing, the proposed method achieves a very ideal effect. The proposed method is applied to MRI images. Among the five methods mentioned above, the nearest neighbor interpolation method is mainly used in medical image processing. Therefore, we use the nearest neighbor method and deep learning combined with the nearest neighbor method in medical image processing. We randomly selected processed image shown in Figure 16.

We can see from the experimental results, the proposed algorithm can achieve amplification function of the image, and the details remain relatively intact, while the nearest

TABLE 7. Comparison of experimental results.

A	INTER	FCN	B	INTER	FCN
	_NEAREST	+INTER		_NEAREST	+INTER
MSE	0.0647	0.00086	MSE	0.0045	0.00012
PSNR/dB	11.8891	30.6777	PSNR/dB	23.4922	39.1726

neighbor interpolation method makes images appear fuzzy, very poor.

To further verify the effectiveness of the algorithm, we perform statistics on MSE and PSNR, as shown in Table 7.

From Table 7, we can find that the proposed algorithm is better than the traditional interpolation algorithm in both MSE and PSNR, which lays a foundation for providing high-quality magnified images for medical diagnosis in the future.

V. CONCLUSION AND DISCUSSION

In order to obtain better reconstruction effect, the model of FCN in this paper introduces the traditional interpolation method into the network to speed up the convergence speed and improve the reconstruction quality while reducing the network parameters. The algorithm proposed in this paper does not need to carry out interpolation and amplification and other preprocessing operations for low-resolution images to be reconstructed before input, and the network can learn more detailed features of images by using deconvolution to complete up-sampling. Compared with other algorithms, the experimental results show that this algorithm is advanced and effective. In the future research, we can try to conduct further research on such aspects as reducing model parameters and improving portability while ensuring the reconstruction quality, in order to realize the reconstruction task on the embedded system with limited memory but fast running speed.

In the next stage, we will expand the training samples, improve the network structure, increase the network depth, and make full use of GPU to reduce the training time and improve the effect.

REFERENCES

- [1] C. Shengda, "The comparison and analysis of several magnification of image magnification," *J. Jinhua Polytech.*, vol. 12, no. 3, pp. 66–70, 2012.
- [2] K. Jensen and D. Anastassiou, "Subpixel edge localization and the interpolation of still images," *IEEE Trans. Image Process.*, vol. 4, no. 3, pp. 285–295, Mar. 1995.
- [3] D. D. Muresan and T. W. Parks, "Adaptively quadratic (AQua) image interpolation," *IEEE Trans. Image Process.*, vol. 13, no. 5, pp. 690–698, May 2004.
- [4] X. Li and M. T. Orchard, "New edge-directed interpolation," *IEEE Trans. Image Process.*, vol. 10, no. 10, pp. 1521–1527, Oct. 2001.
- [5] K.-W. Hung and W.-C. Siu, "Robust soft-decision interpolation using weighted least squares," *IEEE Trans. Image Process.*, vol. 21, no. 3, pp. 1061–1069, Mar. 2011.
- [6] W. Dong, L. Zhang, G. Shi, and X. Wu, "Nonlocal back-projection for adaptive image enlargement," in *Proc. 16th IEEE Int. Conf. Image Process. (ICIP)*, Nov. 2009, pp. 349–352.
- [7] X. Zhang, S. Ma, Y. Zhang, L. Zhang, and W. Gao, "Nonlocal edge-directed interpolation," in *Proc. Pacific-Rim Conf. Multimedia*, Berlin, Germany, Springer, 2009, pp. 1197–1207.

- [8] C. S. Wong and W. C. Siu, "Adaptive directional window selection for edge-directed interpolation," in *Proc. 19th Int. Conf. Comput. Commun. Netw.*, Aug. 2010, pp. 1–6.
- [9] K. Mishiba, T. Suzuki, and M. Ikehara, "Edge-adaptive image interpolation using constrained least squares," in *Proc. IEEE Int. Conf. Image Process.*, Sep. 2010, pp. 2837–2840.
- [10] G. Casciola, L. B. Montefusco, and S. Morigi, "Edge-driven image interpolation using adaptive anisotropic radial basis functions," *J. Math. Imag. Vis.*, vol. 36, no. 2, pp. 125–139, 2010.
- [11] S. Mallat and G. Yu, "Super-resolution with sparse mixing estimators," *IEEE Trans. Image Process.*, vol. 19, no. 11, pp. 2889–2900, Nov. 2010.
- [12] F. Zhou, W. Yang, and Q. Liao, "Interpolation-based image super-resolution using multisurface fitting," *IEEE Trans. Image Process.*, vol. 21, no. 7, pp. 3312–3318, Jul. 2012.
- [13] G. Panchal, A. Ganatra, Y. P. Kosta, and D. Panchal, "Behaviour analysis of multilayer perceptrons with multiple hidden neurons and hidden layers," *Int. J. Comput. Theory Eng.*, vol. 32, pp. 332–337, Apr. 2011.
- [14] A. Dedinec, S. Filiposka, A. Dedinec, and L. Kocarev, "Deep belief network based electricity load forecasting: An analysis of Macedonian case," *Energy*, vol. 115, pp. 1688–1700, Nov. 2016.
- [15] Y. Lecun, B. Boser, and J. S. Denker, "Backpropagation applied to handwritten zip code recognition," *Neural Comput.*, vol. 1, no. 4, pp. 541–551, 1989.
- [16] K. He, X. Zhang, S. Ren, and J. Sun, "Spatial pyramid pooling in deep convolutional networks for visual recognition," *IEEE Trans. Pattern Anal. Mach. Intell.*, vol. 37, no. 9, pp. 1904–1916, Sep. 2015.
- [17] A. Krizhevsky, I. Sutskever, and G. Hinton, "ImageNet classification with deep convolutional neural networks," in *Proc. NIPS*, 2012, pp. 1097–1105.
- [18] W. Ouyang, X. Wang, X. Zeng, S. Qiu, P. Luo, Y. Tian, H. Li, S. Yang, Z. Wang, C.-C. Loy, and X. Tang, "DeepID-Net: Deformable deep convolutional neural networks for object detection," in *Proc. IEEE Conf. Comput. Vis. Pattern Recognit. (CVPR)*, Jun. 2016, pp. 2403–2412.
- [19] N. Zhang, J. Donahue, R. Girshick, and T. Darrell, "Part-based R-CNNs for fine-grained category detection," in *Proc. Eur. Conf. Comput. Vis. Zürich, Switzerland: Springer*, 2014, pp. 834–849.
- [20] Y. Sun, Y. Chen, X. Wang, and X. Tang, "Deep learning face representation by joint identification-verification," in *Proc. Adv. Neural Inf. Process. Syst.*, 2014.
- [21] W. Ouyang and X. Wang, "Joint deep learning for pedestrian detection," in *Proc. IEEE Int. Conf. Comput. Vis. (ICCV)*, Dec. 2013, pp. 2056–2063.
- [22] G. E. Hinton, "Rectified linear units improve restricted Boltzmann machines Vinod nair," in *Proc. Int. Conf. Mach. Learn.*, Madison, WI, USA, Omnipress, 2010.
- [23] H. Chang, D.-Y. Yeung, and Y. Xiong, "Super-resolution through neighbor embedding," in *Proc. IEEE Comput. Soc. Conf. Comput. Vis. Pattern Recognit.*, Jun./Jul. 2004, p. 1.
- [24] X. Gao, K. Zhang, D. Tao, and X. Li, "Image super-resolution with sparse neighbor embedding," *IEEE Trans. Image Process.*, vol. 21, no. 7, pp. 78–85, Jul. 2012.
- [25] R. Timofte, V. De Smart, and L. V. Gool, "Anchored neighborhood regression for fast example-based super-resolution," in *Proc. IEEE Int. Conf. Comput. Vis. (ICCV)*, Dec. 2013, pp. 1920–1927.
- [26] J. Yang, J. Wright, T. S. Huang, and Y. Ma, "Image super-resolution via sparse representation," *IEEE Trans. Image Process.*, vol. 21, no. 7, pp. 2861–2873, Nov. 2010.
- [27] C. Dong, C. C. Loy, K. He, and X. Tang, "Image super-resolution using deep convolutional networks," *IEEE Trans. Pattern Anal. Mach. Intell.*, vol. 38, no. 2, pp. 295–307, Feb. 2014.
- [28] C. Dong, Y. Deng, C. L. Chen, and X. Tang, "Compression artifacts reduction by a deep convolutional network," in *Proc. IEEE Int. Conf. Comput. Vis.*, Dec. 2015, pp. 576–584.
- [29] Y. N. Wang, P. L. Qin, and C. P. Li, "Improved algorithm of image super resolution based on residual neural network," *J. Comput. Appl.*, vol. 22, no. 1, pp. 246–254, 2018.
- [30] J. Kim, J. K. Lee, and K. M. Lee, "Accurate image super-resolution using very deep convolutional networks," in *Proc. IEEE Conf. Comput. Vis. Pattern Recognit. (CVPR)*, Jun. 2016, pp. 1646–1654.
- [31] Y. Li, M. Paluri, J. M. Rehg, and P. Dollar, "Unsupervised learning of edges," in *Proc. IEEE Conf. Comput. Vis. Pattern Recognit.*, Jun. 2016, pp. 1619–1627.
- [32] McGill University. (Mar. 09, 2016.) *Montreal Neurological Institute McConnell Brain Imaging Centre BrainWeb[EB/OL]*. [Online]. Available: <http://brainweb.bic.mni.mcgill.ca/brainweb>.



NA SUN received the Ph.D. degree in signal and information processing from the Beijing University of Posts and Telecommunications, in 2010. She is currently a Lecturer with the School of Information Engineering, Minzu University of China. Her current research interest focuses on parallel algorithm and intelligent systems.



HUINA LI received the M.S. degree in mathematics from Henan University, in 2008. She is currently an Associate Professor with the School of Information Engineering, Xuchang University, China. Her research interests include machine learning, data mining, and image processing.

• • •